

## Reemergent Order of Chaotic Circular Couette Flow

R. W. Walden<sup>(a)</sup> and R. J. Donnelly

*Department of Physics, University of Oregon, Eugene, Oregon 97403*

(Received 4 August 1978)

Measurements of the fluctuations in local velocity in fluid motion between a rotating inner cylinder and a fixed outer cylinder are reported for rotation rates up to  $67R_c$ ,<sup>1</sup> where  $R_c$  is the critical Reynolds number for Taylor instability. The Reynolds number  $R_t$  for which the transition from periodic or quasiperiodic to aperiodic flow occurs depends strongly on aspect ratio ( $\Gamma$  = fluid height/gap):  $R_t \approx 22R_c$  for  $\Gamma = 20$ ;  $R_t \approx 26R_c$  for  $\Gamma = 80$ . For  $\Gamma \gtrsim 25$  a sharp periodic component reemerges in the power spectrum for  $28R_c \lesssim R \lesssim 36R_c$ .

In couette flow between concentric cylinders with the outer cylinder fixed a series of instabilities occurs with slowly increasing rotation rate of the inner cylinder. The fluid motion, which is laminar and parallel to the motion of the inner cylinder for small rotation rates, is transformed to a steady pattern of toroidal rings or "Taylor cells" following the first instability. With increasing stress these rings acquire azimuthal waves and evolve through a series of "states" defined by various combinations of axial and azimuthal wavelength.<sup>1</sup> These waves generate a distinct spectral line with an appropriate detector. At some Reynolds number denoted  $R_t$  all line spectral features disappear; the flow seems to have lost its azimuthal periodicity and in that sense to be disordered.<sup>2</sup> We call the change at  $R_t$  an "aperiodic transition," but caution the reader to recall that axial periodicity persists to the highest Reynolds numbers yet observed. Analogous behavior has been reported for other systems<sup>3</sup> as, for example, in Rayleigh-Bénard convection.

We now find, however, that for sufficiently large aspect ratio  $\Gamma = L/d$  ( $L$  = fluid height;  $d = R_2 - R_1$  = gap between cylinders) a sharply defined azimuthal wave reemerges for inner cylinder rotation rate well beyond the "aperiodic transition" at  $R_t$ . Further, the aspect ratio greatly influences the rotation rate for which the aperiodic transition occurs and the set of possible states accessible to the system immediately below the transition.

The apparatus for our experiments consists of two pairs of cylinders of nearly identical physical dimensions—one pair for visual observations and the other for electrical measurements. In each case the inner cylinder radius is  $R_1 = 2.2225 \pm 0.0003$  cm, and the outer cylinder radius is  $R_2 = 2.5383 \pm 0.0005$  cm. The lower fluid boundary is a stationary brass ring which fills the fluid

gap, except for a  $6.4 \times 10^{-3}$ -cm gap between the inner cylinder and the ring. The upper boundary is a free surface. Visual observations have been made through a glass outer cylinder with fine aluminum flakes (aluminum paint pigment) suspended in the working fluid (carbon tetrachloride).

Electrical measurements are made using a pair of gold-plated brass cylinders. The outer cylinder has an array of 1500 ion collectors from which any four may be connected for computer sampling at a given time. The 1-mm-diam ion collectors produce an output current of the order of 0.1 picoampere and provide a *local* probe ( $\sim 5 \times 10^{-5}$  cm<sup>3</sup>) of the radial component of fluid velocity in a narrow boundary layer at the outer cylinder.<sup>4</sup> The entire apparatus is enclosed in a wooden box which maintains temperature constant to  $\pm 0.1^\circ$  C, and inner-cylinder rotation rate is locked to a programmable synthesizer which maintains constant speed to better than  $\pm 0.01\%$  or permits uniform acceleration at any convenient rate under computer control.<sup>5</sup>

The Reynolds number  $R = 2\pi\Omega R_1 d/\nu$  (where  $2\pi\Omega$  = inner cylinder rotation rate,  $\nu$  = kinematic viscosity, and  $d = R_2 - R_1$ ) will serve as a dimensionless measure of rotation rate in the following discussion.  $R_c = 118.3$  is the critical Reynolds number for the onset of Taylor cells.

For the experiments reported here aspect ratio  $\Gamma$  has ranged from 18 to 80, and data have been taken for Reynolds numbers up to  $R \approx 67R_c$ . The observable set of "states" accessible to the system as  $R$  is increased through  $R_t$  has been described in Refs. 1 and 2. One example is shown in Fig. 1. The spectral peaks denoted  $\omega_1$  and  $\omega_3$  scale roughly with cylinder rotation frequency  $\Omega$ ; the ratio  $\omega_1/\omega_3$  varies slowly as a function of  $R$  as reported by Fenstermacher *et al.*<sup>6</sup> As the aspect ratio  $\Gamma$  is increased,  $R_t$  increases and the ranges over which spectral features such as  $\omega_1$  and  $\omega_3$  are present change. For example, Fig. 1

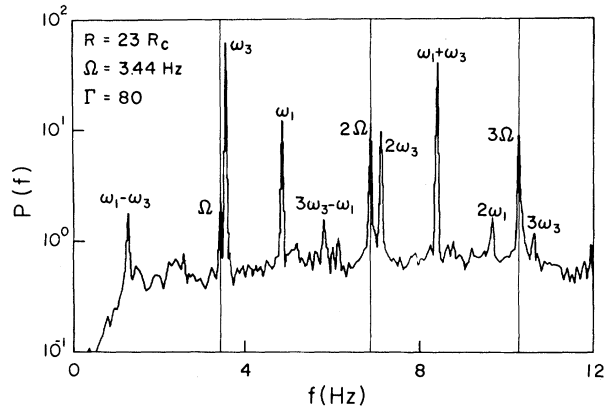


FIG. 1. Power spectrum for which  $\omega_1$  and  $\omega_3$  are present as well as many harmonics and difference frequencies. Spectral peaks at the cylinder rotation speed and its harmonics are artifacts of minute periodic changes in capacitance between the rotating inner cylinder and the ion collector mounted in the outer cylinder. Unlike the other peaks they are present without the fluid.

illustrates data taken for  $\Gamma = 80$  and  $R = 23R_c$ , a Reynolds number which is just beyond the aperiodic transition observed with  $\Gamma = 20$ .

Figure 2 shows data taken for the same aspect ratio  $\Gamma = 80$  and near the same Reynolds number as that displayed in Fig. 1, but it represents a different "state" of the system. When a bifurcation in the flow leads to the appearance of  $\omega_1$  as  $R$  slowly increases, we find that the fundamental frequency first emerges followed by higher harmonics. Conversely, as the system approaches  $R_t$ , the higher harmonics decline in amplitude until at last the fundamental fades into the background spectrum as shown in Fig. 2. Once the system enters a particular state, that state seems to persist for an indefinite period of time as the Reynolds number is varied slowly over a moderate range. However, no well-defined reliable procedure for initiating one or another of the "accessible states" of the system has been determined.

Beyond the Reynolds number  $R_t$  for which the last sharp spectral peak fades from view is a region of apparently disordered fluid motion, although the faint outline of Taylor cells persists in visual experiments to extremely great  $R$ , and the broad spectral feature denoted "B" in Figs. 2 and 4 likewise persists for the largest Reynolds numbers ( $R \approx 67R_c$ ) for which data have been taken. However, for sufficiently large aspect ratio ( $\Gamma \geq 25$ ), a new sharp spectral peak emerges for Reynolds number  $R_r \approx 28R_c$  and persists to Reyn-

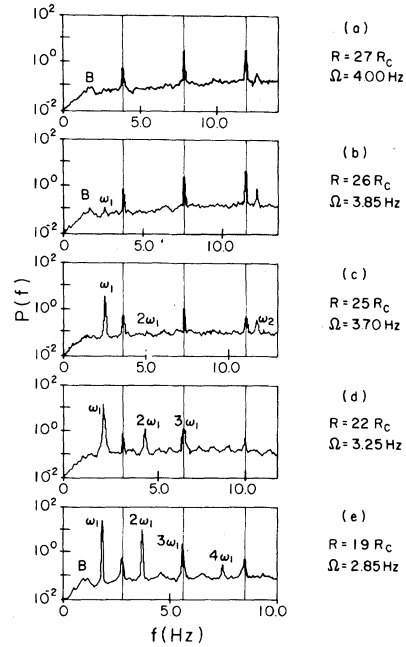


FIG. 2. Power spectral density (on a logarithmic scale) as a function of frequency. The abscissa scale has been normalized to the rotation speed for each plot.  $\omega_1 = 0.68\Omega$  appears with many harmonics at  $R = 19R_c$ ; as  $R$  is increased the higher harmonics and finally the fundamental disappear from the power spectrum.  $\Gamma = 80$ .

olds numbers as great as  $36R_c$ . This new peak has a frequency which scales very closely (within experimental resolution) with cylinder rotation speed  $\Omega$  [ $\omega_r = (1.435 \pm 0.005)\Omega$ ]. The scale factor (1.435) is constant for all data taken with  $\Gamma = 40$  and  $\Gamma = 80$  but appears to increase slightly (by less than 1%) for  $\Gamma = 28$ . (By contrast, the scale factor varies slowly with  $\Omega$  for peaks below the aperiodic transition.

Figure 3 presents a summary of the information above. The upper boundary of region I marks the critical Reynolds number  $R_c$  for the Taylor transition; the boundary above it represents the transition to time-dependent "wavy" modes observed by Cole.<sup>7</sup> Note that the Taylor transition is not much affected by aspect ratio unless there are only a very few cells; but the onset of azimuthal (wavy) modes occurs at considerably higher  $R$  for short aspect ratio. End effects appear to play a similar role in determining the upper cutoff  $R_t$  of the sharp azimuthal modes. As indicated previously, there are often several possible alternative states accessible to the system for a given  $R \leq 27R_c$ . The Reynolds number  $R_t$  for which the sharp spectral peaks vanish as  $R$

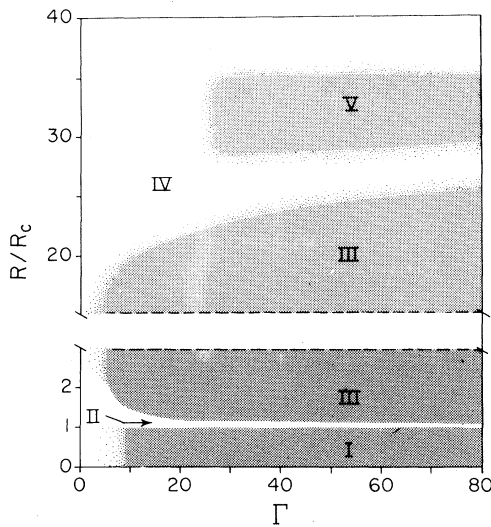


FIG. 3. Domains of various flow states for circular Couette flow: (I) two-dimensional laminar flow; (II) three-dimensional time-independent Taylor flow; (III) time-periodic and quasiperiodic azimuthal (wavy) modes; (IV) aperiodic flow; (V) reemergent peak,  $\omega = 1.44\Omega$ . Not illustrated is the domain of the broad spectral peaks which appear at Reynolds numbers (sometimes) as  $11R_c$  and persist well beyond the top of the diagram for all aspect ratios studied.

increases depends on the initial state of the system. The dashed line denoting the upper limit of the wavy-mode region (III) thus indicates the maximum  $R$  for which *any* sharp spectral modes have been observed. Similarly the dashed boundary of the region (V) for which a sharp spectral peak reemerges denotes the limits within which that peak *may* appear. Several experimental runs with aspect ratios of 20, 28, 40, 56, and 80 probed this reemergent region both by slowly increasing the Reynolds number ( $R^{-1}\Delta R/\Delta t \sim 0.02\%/sec$ ) between data sets and by starting at a very-high Reynolds number ( $R \sim 60R_c$ ) and slowly reducing  $R$ . In some instances the reemergent peak was present throughout the entire range of  $R$  indicated, but at other times (with ostensibly identical test protocol) it persisted through only part of the range.

Figure 4, which displays power spectra for data taken simultaneously at four different points, provides a clue as to why the reemergent peak would not have been observed in an earlier experiment for which  $\Gamma \approx 20$ .<sup>2</sup> Near the center of the fluid depth the peak is quite distinct, but closer to the end of the annulus the amplitude declines until it is no longer discernible above the background spectrum. The same is true near the

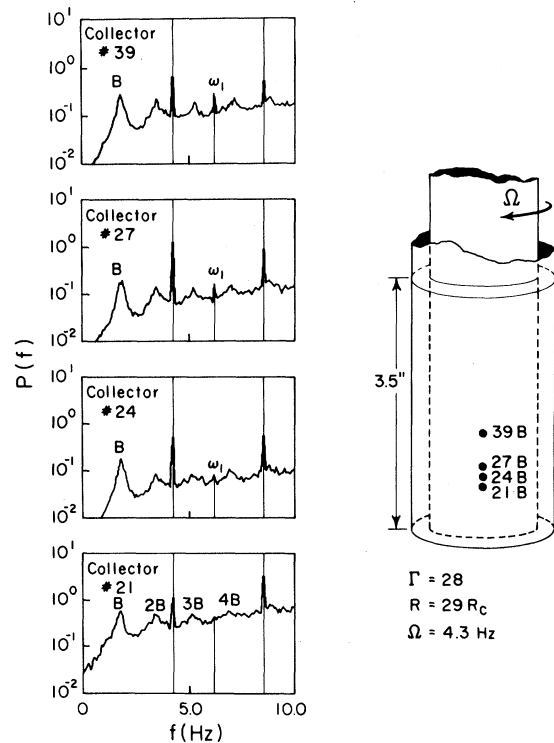


FIG. 4. Power spectral densities recorded simultaneously at the four collectors illustrated on the right. For this aspect ratio,  $\Gamma = 28$ , there is a clear dependence of the amplitude of  $\omega_1$  on the collector position. (Amplitude of  $\omega_1$  has also been observed to decline for collector approaching the upper fluid boundary.)

upper liquid surface. Evidently, then, end effects play a significant role in short-aspect-ratio experiments.

The experimental results reported here leave many more questions to be answered. The re-emergence of a sharp peak in the power spectrum after a range of Reynolds numbers of apparent disorder has not been predicted and suggests that region (IV) of Fig. 3 is really a region of "latent order." If so, is the order still observable in some fashion in the absence of sharp spectral peaks? Current models for the transition from laminar flow to turbulence<sup>8</sup> do not offer many clues.

Comparison of our results with the observations of Ahlers and Behringer<sup>9</sup> for Rayleigh-Bénard convection presents another enigma. Although a series of flow transitions similar to that observed for circular Couette flow is reported for the Rayleigh-Bénard experiment, changing aspect ratio has opposite effects for the two experiments in determining the range over which

time-independent flow and time-periodic flow occur. In the limiting case of very large aspect ratio for the convection experiment, only time-dependent aperiodic flow is observed when convection is initiated, while for circular couette flow the greatest range of periodic states occurs for large aspect ratio.

This research has been supported by the National Science Foundation Grant No. ENG-76-07354.

<sup>(a)</sup>Current address: Bell Laboratories, Murray Hill, N. J. 07974.

<sup>1</sup>See, e.g., D. Coles, *J. Fluid Mech.* **21**, 385 (1965); H. A. Snyder, *Int. J. Non-Linear Mech.* **5**, 659 (1970).

<sup>2</sup>P. R. Fenstermacher, H. L. Swinney, S. V. Benson, and J. P. Gollub, in *Bifurcation Theory and Application in Scientific Disciplines*, edited by O. Gurel and O. E. Rossler (New York Academy of Sciences, New York,

1978); J. P. Gollub and H. L. Swinney, *Phys. Rev. Lett.* **35**, 927 (1975).

<sup>3</sup>See, e.g., J. B. McLaughlin and P. C. Martin, *Phys. Rev. A* **12**, 186 (1975); G. Ahlers and R. P. Behringer, *Phys. Rev. Lett.* **40**, 712 (1978); C. Normand, Y. Poineau, and M. G. Velarde, *Rev. Mod. Phys.* **49**, 581 (1977); J. P. Gollub, T. O. Brunner, and B. G. Danly, *Science* **200**, 48 (1978).

<sup>4</sup>The ion technique utilizes naturally occurring impurity ions in the fluid; the ion probes and both cylinders are held at ground potential. See R. J. Donnelly and D. J. Tanner, *Proc. Roy. Soc. London, Ser. A* **283**, 520 (1965).

<sup>5</sup>For a detailed description of the apparatus, see R. W. Walden, Ph.D. thesis, University of Oregon, 1978 (unpublished).

<sup>6</sup>Fenstermacher *et al.*, Ref. 2.

<sup>7</sup>J. A. Cole, *J. Fluid Mech.* **75**, 1 (1976).

<sup>8</sup>P. C. Martin, in *Proceedings of the International Conference on Statistical Physics, Budapest, 1975*, edited by L. Pal and P. Szepfalusy (North-Holland, Amsterdam, 1975).

<sup>9</sup>Ahlers and Behringer, Ref. 3.

## Doppler-Broadening Measurements of X-Ray Lines for Determination of the Ion Temperature in Tokamak Plasmas

M. Bitter, S. von Goeler, R. Horton, M. Goldman, K. W. Hill, N. R. Sauthoff, and W. Stodiek  
*Plasma Physics Laboratory, Princeton University, Princeton, New Jersey 08540*

(Received 3 November 1978)

Ion-temperature results are deduced from Doppler-broadening measurements of the  $K\alpha$  ( $1s-2p$ ) resonance line emitted from heliumlike iron impurity ions in the hot central core of PLT (Princeton Large Torus) tokamak discharges. The measurements were performed using a high-resolution Bragg-crystal spectrometer with a multiwire proportional counter.

The larger tokamaks of the future require new techniques for the measurement of the ion temperature ( $T_i$ ) in the hot central core of the plasma since the standard methods become more difficult with increasing plasma diameters and electron temperatures ( $T_e$ ). Neutral-charge-exchange diagnostics<sup>1</sup> cannot be used for the determination of the central ion temperature when the mean free path for neutral charge exchange is much smaller than the plasma diameter. The line radiation in the vacuum ultraviolet (vuv) region commonly used for Doppler-broadening measurements<sup>2</sup> of  $T_i$  is emitted primarily from the edge of the plasma at higher central electron temperatures. An exception is the recently observed<sup>3</sup> forbidden line of Fe XX although this line will also originate from outer regions of the plasma column when the electron temperature exceeds 2 keV. An alternate method, the determination of  $T_i$  from a measurement of the neutron yield,<sup>4</sup> is

difficult to interpret if the ion-velocity distribution is not Maxwellian. This may occur, for example, during plasma heating by injection of intense neutral deuterium beams. In this paper we demonstrate that the inner-core ion temperature of a tokamak plasma can be determined from Doppler-broadening measurements of suitable x-ray lines emitted from the plasma.

As  $T_e$  increases, a larger fraction of the electromagnetic radiation is emitted in the x-ray region. This radiation consists of a continuous bremsstrahlung spectrum and characteristic line spectra from high-atomic-number impurity ions, which occur in different degrees of ionization or charge states. In a previous experiment<sup>5</sup> we used a germanium Bragg-crystal spectrometer to investigate the  $K\alpha$ -line spectra of the charge states of iron in Princeton Large Torus (PLT) discharges as a function of  $T_e$ . The measured line intensities and wavelengths were in agree-

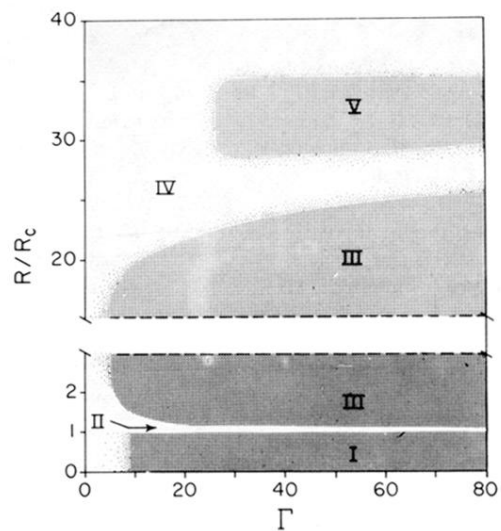


FIG. 3. Domains of various flow states for circular couette flow: (I) two-dimensional laminar flow; (II) three-dimensional time-independent Taylor flow; (III) time-periodic and quasiperiodic azimuthal (wavy) modes; (IV) aperiodic flow; (V) reemergent peak,  $\omega = 1.44\Omega$ . Not illustrated is the domain of the broad spectral peaks which appear at Reynolds numbers (sometimes) as  $11R_c$  and persist well beyond the top of the diagram for all aspect ratios studied.